

Characteristics of Long-Period Microtremors and Their Applicability in Exploration of Deep Sedimentary Layers

by Hiroaki Yamanaka, Masayuki Takemura, Hiroshi Ishida, and Masanori Niwa

Abstract Applicability of long-period microtremors in inferring subsurface structure is examined using measurements of microtremors in the northwestern part of the Kanto Plain in Japan. Short-term continuous measurements of long-period microtremors at both sediment and basement sites were taken. A spectral peak at a period of 4 to 5 sec is stable with time, while peaks at periods less than 2 sec are time variant, suggesting a variation of microtremor sources. However, it was found that the spectral ratio between vertical and horizontal microtremors (ellipticity) at each site is stable with time. Good agreement was found between ellipticities of microtremors at the sediment site and those computed for Rayleigh waves in which the structure of the sediments beneath the site was taken into account. We also found that the ellipticities of Rayleigh waves in earthquake ground motions were consistent with those of the microtremors. These comparisons provide strong evidence that long-period microtremors in the area studied consist mainly of Rayleigh waves. The ellipticity of microtremors was investigated by observing microtremors at temporary observation sites in the Kanto Plain where the sediment thickness varied from 0 to 1 km. The subsurface structures were deduced by trial-and-error fitting of observed ellipticities with theoretical ellipticities that were calculated assuming Rayleigh waves. These results show that ellipticity of long-period microtremors is effective for deducing structure from microtremor data at a single site.

Introduction

The importance of estimating long-period strong ground motion is increasing with recent construction of large-scale man-made structures. Many studies have been conducted to understand characteristics of long-period motion from both observational and theoretical aspects (e.g., Lui and Heaton, 1984; Yamanaka *et al.*, 1992a). These results indicate that long-period earthquake ground motion is often excited in a sedimentary basin and can be interpreted as surface waves amplified in the basin. Because the amplification is significantly influenced by irregularities of a basin, the effect of subsurface irregularities must be accounted for in numerical simulations of strong ground motion. Numerical reconstructions of observed long-period ground motions have been attempted by considering complex irregular structures of basins (e.g., Vidale and Helmberger, 1988; Yamanaka *et al.*, 1992a). Recently, three-dimensional numerical simulations of seismic-wave propagation were examined (Frankel and Vidale, 1992; Toshinawa and Ohmachi, 1992; Motosaka *et al.*, 1992). Although complete amplification of seismic waves can be calculated for a basin with three-dimensional structure, obtaining satisfactory

agreement with measured seismograms is still difficult, partly because of insufficient knowledge of the detailed subsurface structure (Frankel and Vidale, 1992).

In order to achieve a better understanding of long-period ground motion, a model for the subsurface structure must therefore be obtained. Seismic explorations are one of several methods to determine a subsurface structural model over a wide area, but these explorations are still economically and technically difficult to make, especially in urbanized areas. An alternative and easier method is to make microtremor measurements. The application of microtremors to earthquake engineering problems was initiated by Kanai and his colleagues (Kanai and Tanaka, 1961). However, their study was limited to microtremors in a period range of less than 1 sec. Because of the importance of long-period content in strong-motion records, seismologists and engineers should consider using long-period microtremors to assess subsurface structures.¹

¹We note that long-period microtremors are the same as microseisms.

Ohta *et al.* (1978) found good correlation between the thickness of sediments and the predominant period of microtremors in a period range of 1 to 5 sec. A similar correlation was proposed by Kanai and Tanaka (1961) for the analysis of short-period microtremors. It is, however, often difficult to estimate a predominant period that reflects subsurface ground conditions. In such cases, the spectral ratio of long-period microtremors at sites on sediments to that at sites on rocks can be examined instead. Kagami *et al.* (1982) and Akamatsu *et al.* (1992) estimated amplification factors in deep sediments by taking spectral ratios of microtremors. This approach can be valid when long-period microtremors in an area originate from the same source. Akamatsu *et al.* (1992) and Yamanaka *et al.* (1993) showed through continuous observations of long-period microtremors that a possible source is an oceanic disturbance, and that a spectral ratio is much more stable with time than the spectral amplitude of microtremors.

Because the above approaches based on the spectral ratio technique are relatively simple and allow us to directly estimate ground vibrational characteristics of deep sedimentary layers, they are very effective in practical engineering use. However, they are not sufficient for quantitatively interpreting the nature of microtremors. Kudo *et al.* (1976) and Shiono *et al.* (1979) investigated the nature of microtremors through array measurements of microtremors, and found that Rayleigh waves significantly contribute to the vertical component of long-period microtremors. Using array data of long-period microtremors, Horike (1985) and Matsushima and Okada (1990) estimated the structure of the *S*-wave velocity in deep sediments by inversion of the phase velocity of Rayleigh waves. Although we can estimate subsurface structure from array measurements, the measurements are difficult to make.

In this study, we observed long-period microtremors in the northwestern part of the Kanto Plain, Japan, to investigate the nature of long-period microtremors and to assess their use for determining subsurface structure. We set up ten observation stations on firm rocks and on deep sediments along a 12-km band. At one of the stations, HMY, a strong-motion observation was conducted (Omote *et al.*, 1980) and various characteristics of strong-motion records were investigated (e.g., Muto *et al.*, 1982). Using records from the strong-motion observation, we interpreted characteristics of long-period microtremors by comparing the earthquake and microtremor records.

Subsurface Structure in the Investigated Area

Figure 1 shows the surface geological setting for the ten observation sites located in the northwestern region of the Kanto Plain. The western portion of the area is mountainous, showing an outcrop of hard rocks. The crystalline schist is a metamorphic rock formation in the

Chichibu system from either the Mesozoic or Paleozoic age. The eastern portion is covered by Tertiary and Quaternary sediments. The surface geology of our observation area suggests that tectonic lines exist near the basement/sediment boundary. One of the major lines is the Hachiohji line, running in the north-south direction (Koiki *et al.*, 1985). A gravity survey (Hagiwara *et al.*, 1987) revealed that toward the east of the Hachiohji tectonic line the basement rapidly deepens from 0.1 to 1.0 km within a distance of a few kilometers.

Seismic surveys of the area revealed the velocity profiles. Muto *et al.* (1982) obtained the profiles for *P* and *S* waves beneath the earthquake observation site at HMY using unreversed explosion data, and estimated the depth to the basement as 1.3 km. Seo *et al.* (1990) analyzed dense reversed refraction data for the area east of HMY. Using the *P*-wave velocity profiles obtained by Seo *et al.* (1990), Yamanaka *et al.* (1992b) obtained a profile for the *S* waves beneath the HMY site from a dispersion analysis of earthquake records.

Observation and Instruments

Our observation of long-period microtremors was carried out in May 1992, using two types of measurements: continuous measurements at two sites, and temporary measurements at eight sites. In the continuous measurements, we installed instruments at two sites about 10 km apart, one is a rock site (designated as OGW in Fig. 1) and one is a sediment site (HMY), in order to determine the stability of the microtremors. The measurements of microtremors were continuously taken every 2 hr, starting in the evening and ending the next morning, totaling seven synchronized recordings.

After completion of the continuous measurements at the two sites, temporary measurements were taken at eight stations located along a 12-km line between OGW and HMY (see Fig. 1). As can be seen in Figure 1, sites 1 and 2 are rock sites, and the others are sediment sites. Because we prepared only two sets of instruments, one set was used for the temporary measurements and the other was installed at HMY to continue taking the continuous measurements to examine the stability of microtremors during the temporary measurements. The measurements at HMY were continued every 2 hr until the temporary measurements were finished.

The observational system consisted of three seismometers, two for the horizontal components and one for the vertical component (Project Team for the Development of Small-Size Long-Period Seismometer, 1974), an amplifier, and a digital recorder. The natural period of each seismometer was set at 10 sec. After amplifying the ground velocity from the seismometer, a high-cut filter with a cutoff frequency of 10 Hz was applied. Then, the record was sampled every 0.02 sec with an accuracy of 12 or 14 bits. Each recording consisted of

10 min of data on the horizontal and vertical components of the microtremors.

Results of the Microtremor Measurements

Results of the Continuous Measurements

The stability of microtremors must be confirmed before an accurate interpretation of microtremor data can be made. We therefore investigated the stability of microtremors by using data from the continuous measurements on the basement at OGW and on the sediments at HMY.

Examples of the horizontal components of microtremor records observed at OGW and HMY are shown in Figure 2. The amplitudes of the records at OGW are smaller than those at HMY, suggesting different geological strata. We note that the records at 6:00 at the two sites have amplitudes several times larger than those at the other times and are rich in longer-period content. Although records in the vertical and EW components are not shown in Figure 2, we can also identify similar characteristics in those records. The records observed at 8:00

and 10:00 exhibit similar characteristics to those before 4:00. Therefore, instrument-related causes cannot be attributed to these records. It turned out that a moderate earthquake occurred in the Pacific Ocean at 5:40 several hundred kilometers south of the measurement sites, and had a magnitude of 5.5 and a focal depth of 25 km (Japan Meteorological Agency, 1992). The records obtained at 6:00 are therefore due to coda waves from the distant earthquake.

Next, we calculated Fourier spectra from the records. The spectra were calculated using FFT on data having a duration of 163.84 sec. The Parzen spectral window with a bandwidth of 0.1 Hz was applied to smooth the spectra. Because there were no significant differences in the two horizontal spectra, they were geometrically averaged to generate a single horizontal spectrum. We calculated three spectra from three segments in an original record observed at each site at each observation time. The spectra were then averaged.

Examples of the spectra of the microtremors at OGW and HMY are displayed in Figure 3. Except for the spectra at 6:00, all the spectra at OGW in Figures 3a and 3d show similar characteristics, having a single spectral peak

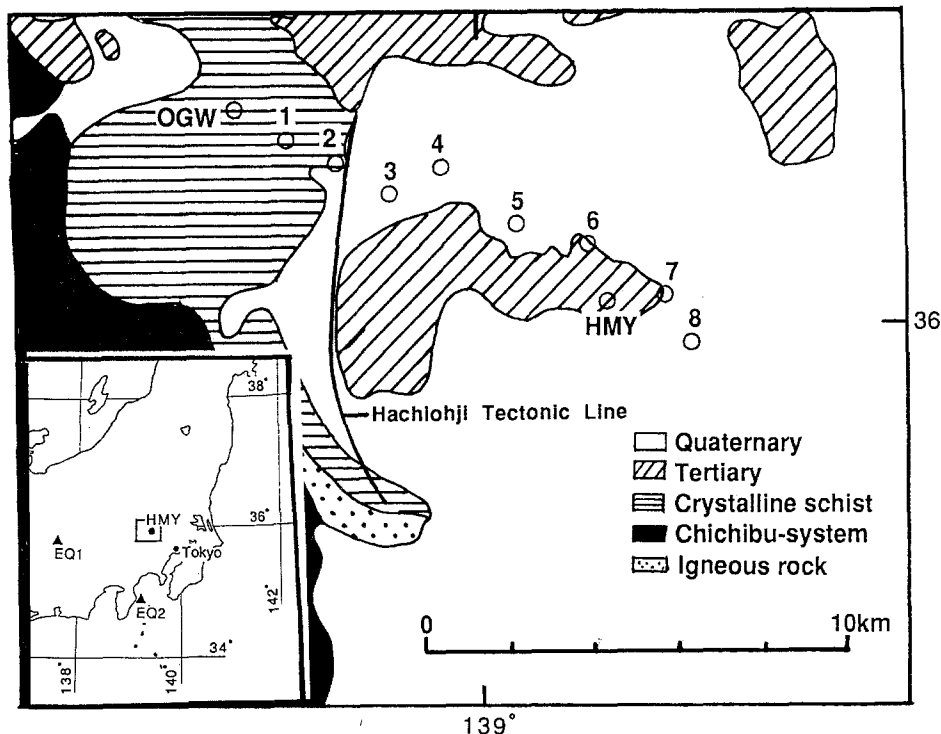


Figure 1. Map of the northwestern region of the Kanto Plain, Japan, showing locations of microtremor observation sites with surface geological conditions. The western part of the area is a mountainous region, and sediments thicken toward the east. The solid line shows the location of the Hachiohji tectonic line (Koike *et al.*, 1985). The triangles are epicenters of two earthquakes: EQ1 is the western Nagano earthquake that occurred on 14 September 1984 with an M_{JMA} of 6.8, and EQ2 is the Off Izu Peninsula earthquake that occurred on 29 June 1976 with an M_{JMA} of 6.7. Continuous measurements were taken at the HMY and OGW sites, and temporary measurements at stations 1 through 8.

in a period range from 4 to 5 sec. The spectra at HMY in Figures 3b and 3e also have a similar spectral peak, but with amplitudes larger than those at OGW. In addition to the common spectral peak, we can see two spectral peaks at periods of about 1.5 and 0.3 sec in the spectra at HMY. The spectral peak at a period of 0.3 sec is

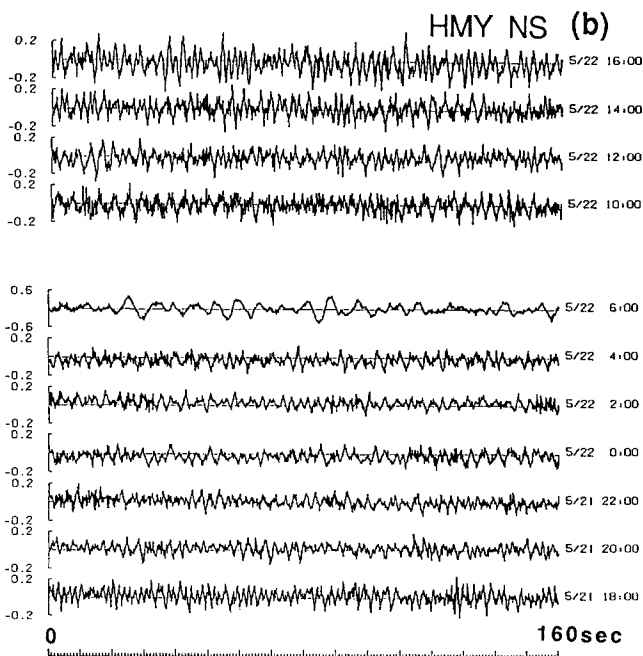
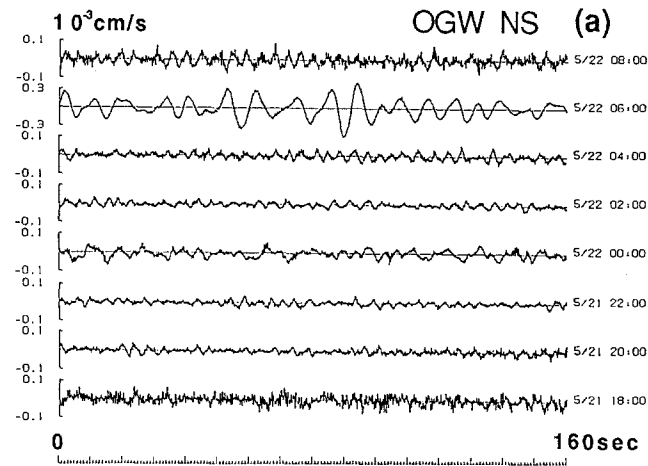


Figure 2. Examples of microtremor records at (a) OGW and (b) HMY on 21 and 22 May 1992. Each trace indicates north-south ground velocity. Note that the records at 6:00 differ because of the coda waves of a distant 5.5-magnitude earthquake that occurred several hundred kilometers south of the observation sites.

probably caused by human activities, such as traffic and industrial activities. In contrast to other observation times, the spectra for the coda waves at 6:00 at both sites have a predominant period of about 10 sec and an amplitude ten times larger. Because these features for the coda waves are identified in the spectra at both HMY and OGW, we conclude that they are caused by source effects and/or global path effects.

After the instrument at OGW was removed for the temporary measurements, we continued the continuous measurements at HMY every 2 hr for 6 hr. Figures 3c and 3f show the spectra observed at HMY taken during the same time period as the temporary measurements. A spectral peak can still be found between a period of 4 to 5 sec. However, during this 6-hr period, the other spectral peaks at periods shorter than 2 sec are unstable, showing time-variant peak periods. This can be due to a variation of a microtremor source. We note that the weather conditions during the temporary measurements were very unstable and that we had a short thunderstorm in the afternoon. This sudden environmental change might have produced such an unstable microtremor spectra in the shorter-period range. Because the spectra in this range were unstable, corrections were required in the analysis of the microtremor data obtained in the temporary measurements.

Results of Temporary Measurements

Temporary measurements were taken at the eight stations, starting from station 1 near OGW on the basement to station 8 on the sediments near HMY. The Fourier spectra of the data obtained at these stations are shown in Figure 4. The spectra at stations 1 and 2 on the basement have the same characteristics as those for OGW; namely, a single peak between a period of 4 to 5 sec. This peak can also be found in the spectra at the other stations on the sediments. The amplitudes at this period at the sediment sites are larger than those on the basement in the horizontal component, but are almost the same as those in the vertical component. Additional spectral peaks are identified at periods shorter than 2 sec at the sediment sites. The periods of these peaks become longer at the stations further east, where the sediment thickness increases. However, we cannot identify whether or not the spectral variation in this period range reflects differences in ground conditions, because the spectral characteristics of microtremor sources in this period range are time dependent.

Ellipticity of Microtremors

Array analysis of microtremors suggested that microtremors are composed of surface waves (e.g., Horike, 1985; Matsushima and Okada, 1990). When observed microtremors consist mainly of Rayleigh waves, a spectral ratio of vertical and horizontal components at a sin-

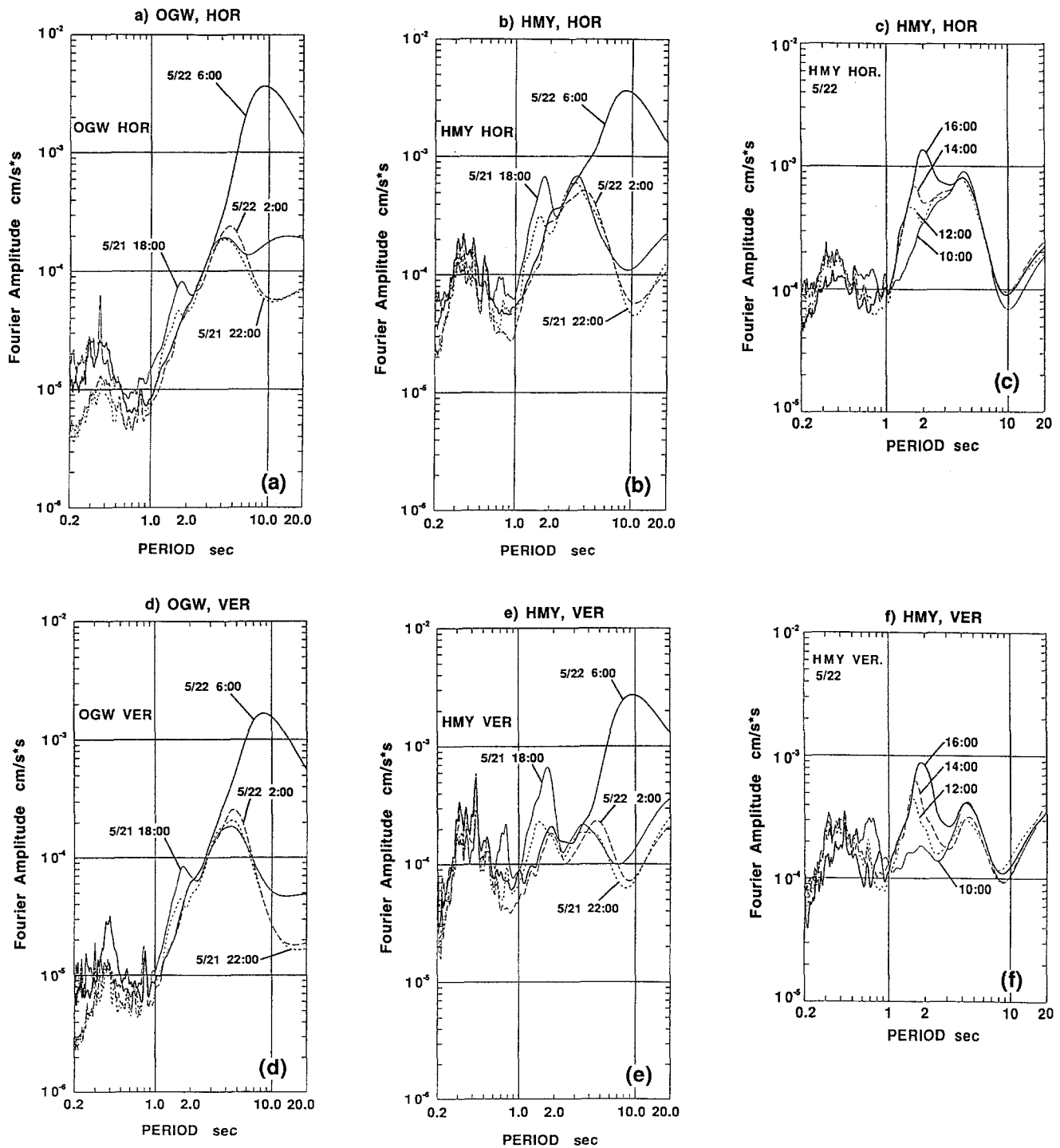


Figure 3. Examples of Fourier spectra of microtremors observed at OGW and HMY. Spectra for the horizontal components at (a) OGW and (b) HMY during the continuous measurements. (c) Spectra for the horizontal components at HMY taken during the same time period as the temporary measurements. Spectra for the vertical components at (d) OGW and (e) HMY during the continuous measurements. (f) Spectra for the vertical components at HMY taken during the same period as the temporary measurements. Horizontal spectra are the geometric mean of the NS and EW components.

gle site (ellipticity) has a shape depending only on the subsurface structure beneath the site. For earthquake data, Boore and Toksöz (1969) applied the ellipticity of Rayleigh waves to infer subsurface structure. In our study, we investigate the ellipticities of the microtremors at OGW and HMY.

First, we examined the stability of the ellipticity by using the continuous measurement data from OGW and HMY. The ellipticities of the microtremors at different observation times were calculated from spectra for the vertical and horizontal components, and are shown in Figure 5. Because the ellipticities are not time dependent, ellipticity is a stable parameter for interpreting microtremor data. The ellipticity of HMY has a spectral peak at a period of about 3 sec, while ellipticity at OGW is flat in a period range of 1 to 6 sec. This difference can be attributed to the different subsurface structures be-

neath the two sites. We note that there is no difference between the ellipticities of the coda waves due to the earthquake observed at 6:00 and the other ellipticities of the microtremors. This suggests that wave types for the coda part of earthquakes and microtremors are similar.

Next, we consider the ellipticity at the HMY site by taking into account the structure of the sediments. The structure of the *P*- and *S*-wave velocity in the sediments beneath the HMY site was obtained by Yamanaka *et al.* (1992b). Considering the subsurface structural data they obtained, we calculated the theoretical ellipticity of fundamental Rayleigh waves for the structural model shown in Figure 9. The theoretical ellipticity indicated by a broken line in Figure 5 satisfactorily explains the observed ellipticity. When the contribution of Love waves to long-period microtremors is larger than that of Rayleigh waves, the observed ellipticity of microtremors significantly dif-

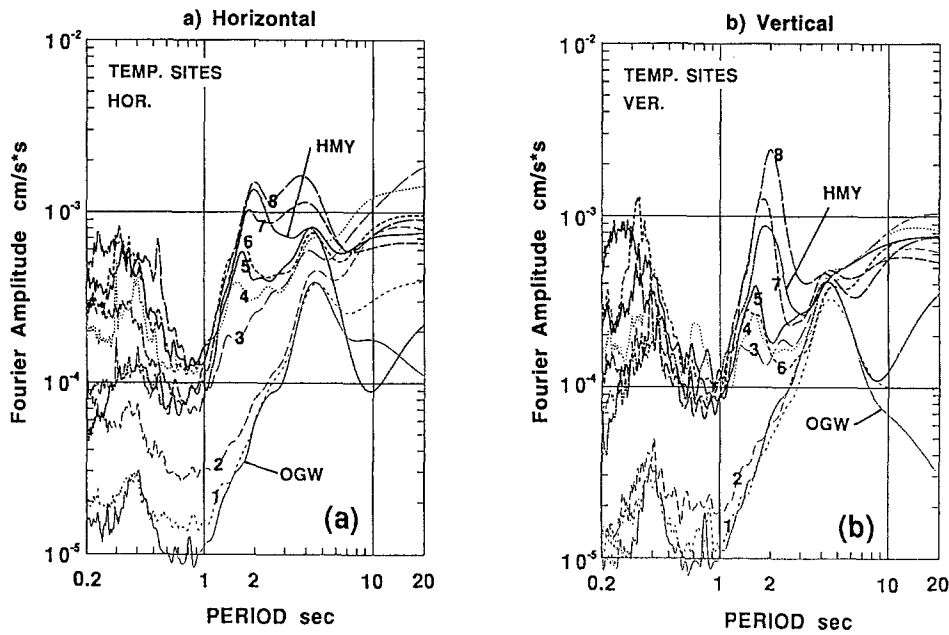


Figure 4. Fourier spectra of (a) horizontal and (b) vertical components of microtremors observed at the temporary observation sites. Horizontal spectra are the geometric mean of the NS and EW components.

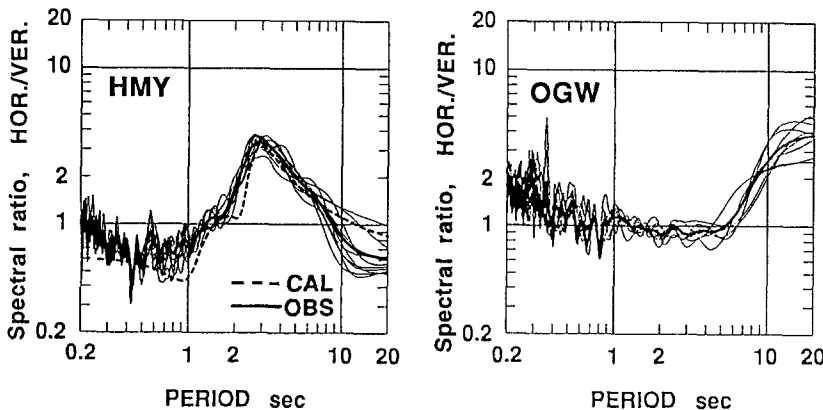


Figure 5. Observed ellipticities of microtremors at (left) HMY and (right) OGW. The thin lines indicate ellipticities observed at each observation time, thick lines the average values, and the broken line the theoretical ellipticity calculated for the fundamental Rayleigh wave in the subsurface structure (shown in Fig. 9) at HMY.

fers from the theoretical values. However, the close agreement clearly indicates that Rayleigh waves are the largest component in the long-period microtremors at HMY.

Comparison between Ellipticities of Earthquake Ground Motions and Ellipticities of Microtremors

Long-period microtremors are generated by oceanic disturbances (e.g., Longuet-Higgins, 1950) and are probably a summation of elementary waves, thus making it difficult to interpret the characteristics of microtremors. Such microtremors are different from Rayleigh waves generated by an explosion or an earthquake, which are easier to interpret. We therefore compare the ellipticities for microtremors (shown in Fig. 5) with the ellipticities for earthquake ground motions to better understand the nature of microtremor ellipticity. Strong-motion earthquake records observed at HMY were used for this comparison.

Two records were selected for the comparison: the western Nagano earthquake that occurred on 14 September

1984 with an M_{JMA} of 6.8, and the Off Izu Peninsula earthquake that occurred on 29 June 1976 with an M_{JMA} of 6.7. The locations of the epicenters of the events are shown in Figure 1 (triangles in the figure). According to previous research on the observed ground motions, long-period surface waves were dominant in the records because of the shallow focal depths and deep sediments beneath the observation site (e.g., Muto *et al.*, 1982; Yamanaka *et al.*, 1992b). The integrated ground velocities observed near the surface (0.6 m below) are displayed in Figure 6 with their corresponding Fourier spectra. The traces in the figure are filtered in a period range from 0.2 to 10 sec, and the horizontal records were rotated in the transverse and radial directions. The dispersive wave trains in the transverse and radial directions are Love and Rayleigh waves, respectively.

We calculated the ellipticity of the Rayleigh waves from the radial and vertical components of the earthquake spectra. The calculated ellipticities are shown in Figure 7, along with those of the microtremors. Although the ellipticities for the earthquake records show scatter, their peak periods and amplitudes are almost the

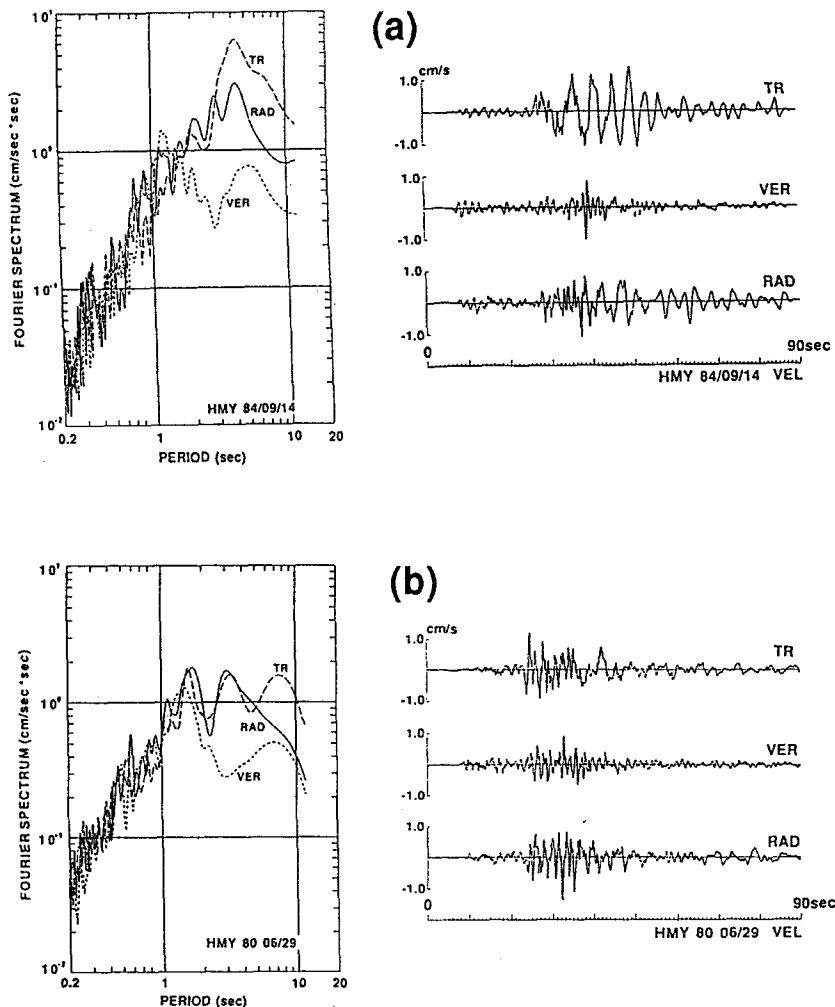


Figure 6. Observed ground velocity records and their corresponding Fourier spectra for station HMY during (a) the western Nagano earthquake on 14 September 1984 at an M_{JMA} of 6.8 and (b) the Off Izu Peninsula earthquake on 29 June 1980 at an M_{JMA} of 6.7. The horizontal components were rotated in the transverse and radial directions.

same as those of the microtremors, particularly in a period range from 1 to 10 sec. This agreement indicates that the long-period microtremors at periods longer than 1 sec were Rayleigh waves.

Estimation of Subsurface Structure from the Ellipticity of Microtremors

We have shown above that the ellipticity of long-period microtremors is stable and can be used as an effective parameter to extract information on subsurface structure. Using the data observed at the temporary observation sites, we now examine the applicability of using microtremor ellipticity for determining subsurface structure. We estimate the thicknesses of the sediments, which vary from 0 to 1 km, by comparing observed and calculated microtremor ellipticities.

In the analysis, we assumed that only the fundamental mode of Rayleigh waves contributes to the ellipticities of microtremors, and that the velocity configuration of sedimentary layers at each site is the same as that at the HMY site, where the velocity profiles were investigated (see Fig. 9). Namely, *S*-wave velocities of 0.7, 1.0, 1.5, and 3.0 km/sec were fixed except for additional top-surface layers having different *S*-wave velocities. We then adjusted the thickness of the sedimentary layers to find a reasonable fit of the calculated ellipticities and observed ellipticities by trial-and-error. In particular, we focused on fitting the peak periods and amplitudes of the ellipticity in a period range longer than about 1 sec.

The observed and calculated ellipticities are shown in Figure 8 with inferred structural models for each site

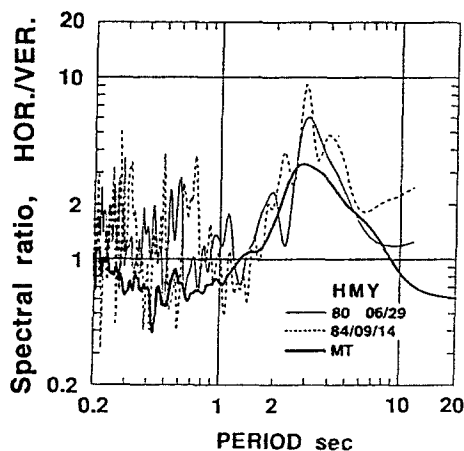


Figure 7. Comparison between the ellipticities for microtremors at HMY with those for the earthquake ground motions shown in Figure 6. The geometric mean of the NS and EW components was used in calculating microtremor ellipticities, while the radial component was used in earthquake ellipticities.

(summarized in Fig. 9). The observed ellipticities at sites 1, 2, and OGW (characterized as rock sites) are similar, i.e., flat in a period range from 0.5 to 6 sec. Although the calculated ellipticity is slightly smaller than the observed ellipticities, the model reproduces the flat characteristics of the observed ellipticities at these rock sites. The peaks at periods of 20 sec seen in the observed ellipticities at sites 1 and OGW were ignored in the fitting of the ellipticities, because our measuring instruments had natural periods of about 10 sec.

The ellipticities at sites 3, 4, and 5, which were located near the boundary of the rock and sediment areas, have small, broad peaks between the periods of 2 and 4 sec. The structural model applied to site 3 produces the same velocities as those at the HMY site, which has a different thickness. Good agreement was obtained in a period range from 0.5 to 10 sec. We deduced the models for sites 4 and 5 by adding top layers to obtain a better fit of the ellipticities at periods shorter than 2 sec. The ellipticities observed at sites 6, 7, 8, and HMY (lower part of Fig. 8) have higher and narrower spectral peaks than those observed at sites 3, 4, and 5. In particular, the peak period becomes longer at site 8. Although the ellipticity at site 6 is not well represented by the model in a period from 1 to 2 sec, the peak period and its magnitude are well represented. Because site 7 has similar ellipticity to that observed at HMY, the same model can be applied to the site. Lastly, the model for site 8 was determined by fitting the ellipticity at periods longer than 2 sec. We found good agreement between the observed and calculated ellipticities. The depth to the basement at site 8 was estimated as 1.55 km and was the deepest of the sites, reflecting the longest peak period of the ellipticities. The peak at a period of 0.6 sec in the ellipticity at site 8 is probably related to structures of the superficial layers. Because we are only interested in the characteristics of the long-period microtremors and relatively deep subsurface structure, we ignored the peak at the period of 0.6 sec in the fitting of the ellipticity.

The estimated depth to the basement determined with an *S*-wave velocity of more than 2 km/sec between OGW and HMY is summarized in Figure 10. The depth suddenly increases between sites 2 and 3, corresponding to the Hachiohji tectonic line. Westward beyond the tectonic line, the sediment thickness gradually increases. The subsurface structure between OGW and HMY was also revealed from a gravity survey taken by Hagiwara *et al.* (1987). They proposed a depth contour for a basement/sediment boundary assuming that the sediment consists of a single layer. Figure 10 shows the good agreement between our estimated basement depth and that estimated by the gravity survey except for the marginal part of the basin. Because spatial filtering is often applied in the analysis of gravity data, the difference seen in the marginal part is unavoidable.

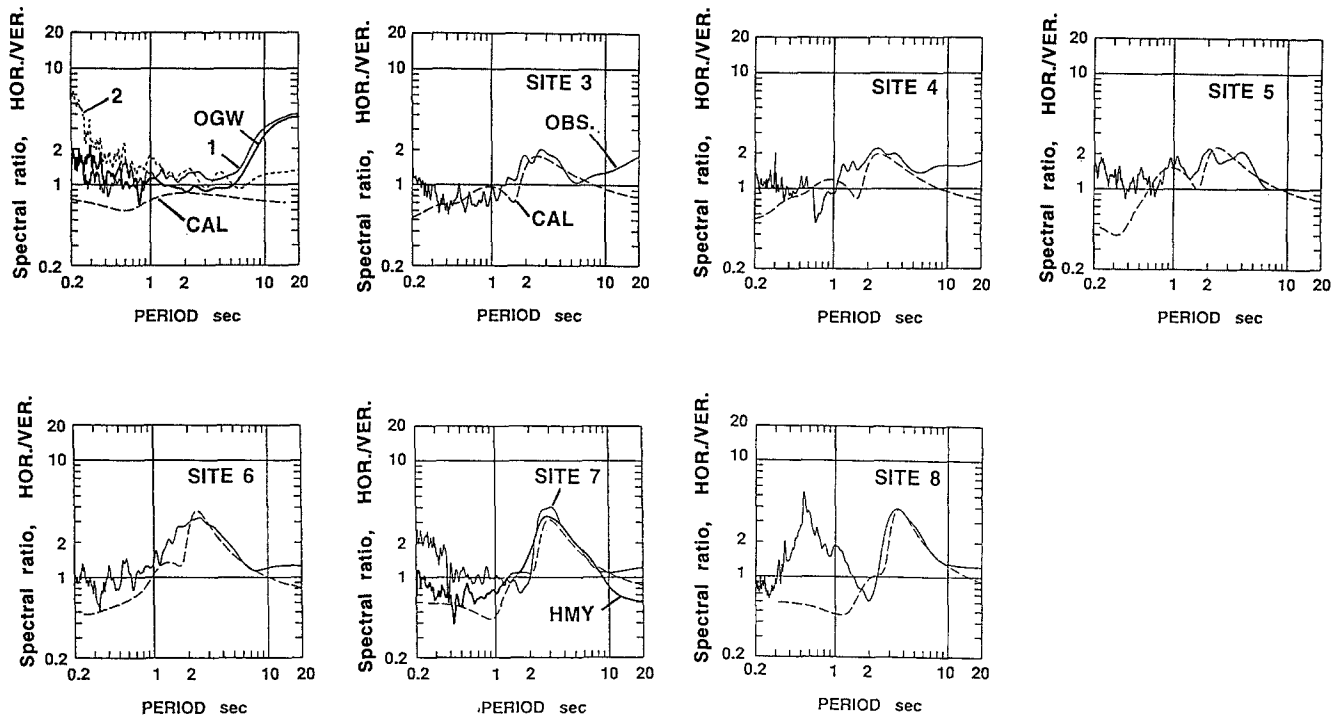


Figure 8. Comparison between the microtremor ellipticities (solid lines) observed at stations 1 through 8 and theoretical ellipticities (broken lines) for fundamental Rayleigh waves in subsurface structures in Figure 9.

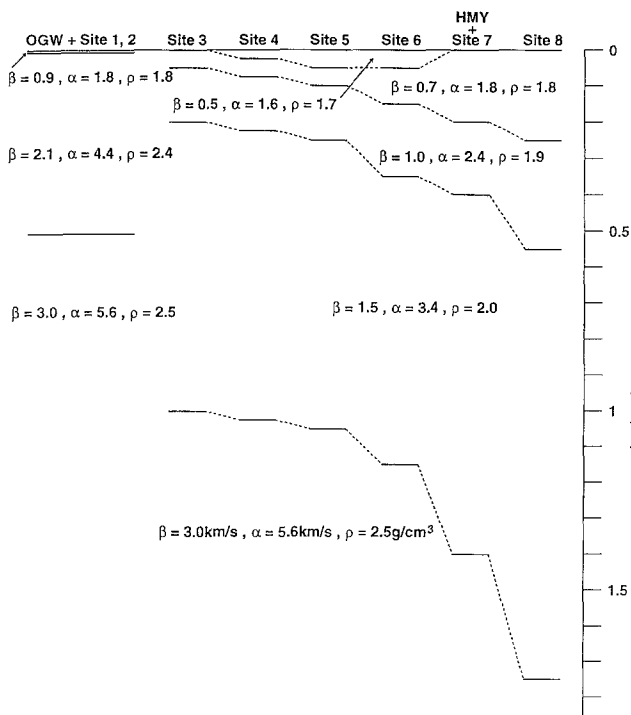


Figure 9. Subsurface structural models for stations 1 through 8 estimated from the comparison shown in Figure 8 between observed ellipticities and calculated ellipticities of Rayleigh waves.

Conclusions

The spectral characteristics of long-period microtremors have been discussed by using the data observed in the northwestern Kanto Plain, Japan. The measurements generated continuous microtremor data at two reference sites, one on a basement and one on sediments,

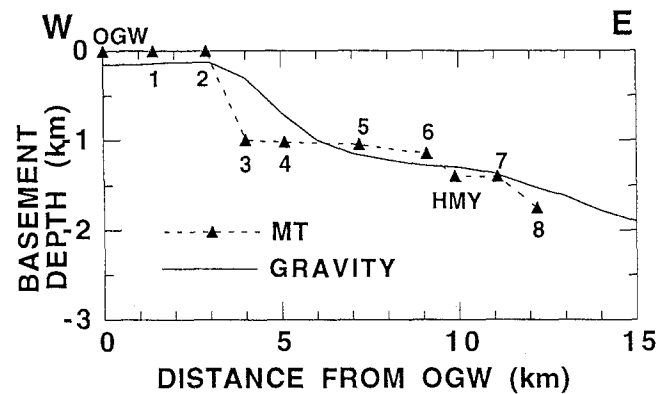


Figure 10. Comparison between the basement depth derived from a gravity survey (Hagiwara *et al.*, 1987) and that from the microtremor ellipticities (MT). Here we define the basement that was deduced from microtremors as a layer having an *S*-wave velocity of more than 2 km/sec.

and microtremor data at eight temporary observation sites (two sites on rocks and six sites on sediments). In every microtremor spectrum, we identified a common and stable peak at a period of 4 to 5 sec and additional time-variant spectral peaks in a period range less than 2 sec, suggesting a complexity of microtremor sources. This time-variant source effect was successfully removed by taking the spectral ratio between the horizontal and vertical components at each site (ellipticity). Good agreement was achieved between the observed microtremor ellipticity at the sediment site, HMY, with the calculated ellipticity for Rayleigh waves, when the structure of the sediments beneath the site was taken into account. The microtremor ellipticity observed at HMY also agreed with those for Rayleigh waves observed at the site during two shallow earthquakes. This agreement between the ellipticities determined from the microtremors, from the earthquake records, and from the calculation involving Rayleigh waves indicates that the microtremors in the observation area were mainly composed of Rayleigh waves. This leads us to use the observed ellipticity to explore subsurface structure. To examine this applicability of microtremor ellipticity, the subsurface structures at the temporary observation sites were deduced by fitting the calculated ellipticities with the observed ellipticities. The estimated structures are coincident with those from a gravity survey.

Even though an array analysis of microtremors is effective for exploring deep sedimentary layers, it requires many stations for a profile. Therefore, we believe that ellipticity measurements of microtremors can be used to deduce profiles at any site by extrapolating a profile at a site obtained from array measurement. However, we assumed in our analysis that the horizontal component of the microtremors consists mainly of Rayleigh waves. We have shown by comparing earthquake and theoretical data that this assumption is acceptable for our investigation. In practical applications, in which no such earthquake and/or structural data are available, we must evaluate the contribution of Love and Rayleigh waves only from microtremor records. A correlation analysis of the vertical and horizontal components of microtremors (e.g., Iyer, 1958) is a possible approach that should be investigated in future work.

Acknowledgments

We are grateful to Etsuzo Shima for valuable advice and critical reading of the manuscript. We thank Hiroyoshi Kobayashi, Kazuoh Seo, and Takanori Samano for fruitful discussions and advice. We are also grateful to Tomonori Ikeura and Takasi Nozawa for their discussions. We thank Alan L. Kafka and an anonymous reviewer for comments on the manuscript. Earthquake records used in this study were provided by the Committee of Strong-Motion Instruments Arrays, which is sponsored by ten Japanese electric power companies.

References

- Akamatsu, J., M. Fujita, and K. Nishimura (1992). Vibrational characteristics of microseisms and their applicability to microzonation in a sedimentary basin, *J. Phys. Earth* **40**, 137–150.
- Boore, D. M. and M. N. Toksöz (1969). Rayleigh wave particle motion and crustal structure, *Bull. Seism. Soc. Am.* **59**, 331–346.
- Frankel, A. and J. Vidale (1992). A three-dimensional simulation of seismic waves in the Santa Clara Valley, California, from a Loma Prieta aftershock, *Bull. Seism. Soc. Am.* **82**, 2045–2074.
- Hagiwara, Y., K. Nagasawa, S. Izutuya, Y. Kotake, and S. Okubo (1987). Gravity study of active faults—detection of faults along the northeastern margin of the Kanto Mountains, *Bull. Earthquake Res. Inst. Univ. Tokyo* **62**, 311–327 (in Japanese with English abstract).
- Horike, M. (1985). Inversion of phase velocity of long period microtremors to the S-wave velocity structure down to the basement in urbanized areas, *J. Phys. Earth* **33**, 59–96.
- Iyer, H. M. (1958). A study on the direction of arrival of microseisms at Kew Observatory, *Geophys. J. R. Astr. Soc.* **1**, 32–43.
- Japan Meteorological Agency (1992). Preliminary report, *Newsletter Seism. Soc. Japan* **4**, no. 2, 35–37 (in Japanese).
- Kagami, H., C. M. Duke, G. C. Liang, and Y. Ohta (1982). Observation of 1- to 5-second microtremors and their application to earthquake engineering. Part II, evaluation of site effects upon seismic wave amplification due to extremely deep soils, *Bull. Seism. Soc. Am.* **72**, 987–998.
- Kanai, K. and T. Tanaka (1961). On microtremors VIII, *Bull. Earthquake Res. Inst. Univ. Tokyo* **39**, 97–114.
- Koike, M., K. Takei, T. Shimono, J. Machida, K. Akimoto, I. Hashiya, H. Yoshino, and S. Hirakoso (1985). Miocene formations of Iwadono hills, *J. Geol. Soc. Japan* **91**, 665–677 (in Japanese).
- Kudo, K., Y. Ohta, N. Goto, H. Kagami, K. Shiono, N. Sakajiri, S. Naruse, K. Izuhara, and F. Takeuchi (1976). Observation of 1- to 5-sec microtremors and their application to earthquake engineering. Part 4, elucidation of propagative characteristics by use of a temporary array net., *Zisin (J. Seism. Soc. Japan)* **29**, 323–337 (in Japanese with English abstract).
- Liu, H. L. and T. Heaton (1984). Array analysis of the ground velocities and accelerations from the 1971 San Fernando California earthquake, *Bull. Seism. Soc. Am.* **74**, 1951–1968.
- Longuet-Higgins, M. S. (1950). A theory of the origin of microseisms, *Philos. Trans. R. Soc. London A* **243**, 1–35.
- Matsushima T. and H. Okada (1990). Determination of deep geological structure under urban areas using long-period microtremors, *Butsuri-Tansa* **43**, 21–33.
- Motosaka, M., M. Kamata, O. Sugawara, and M. Niwa (1992). Surface wave propagation analysis in the Kanto basin. *Proc. 10th World Conf. Earthquake Eng.*, Vol. 2, Madrid, Spain, 19–24 July, 1105–1110.
- Muto, K., T. Ohta, T. Sugano, M. Miyamura, and M. Motosaka (1982). Analysis of earthquake waves observed in strong motion earthquake instruments array, *Proc. 3rd International Conf. on Seismic Microzonation*, Vol. 1, Seattle, Washington, 28 June–1 July, 507–518.
- Ohta, Y., H. Kagami, N. Goto, and K. Kudo (1978). Observation of 1- to 5- second microtremors and their application to earthquake engineering. Part I, comparison with long-period accelerations at the Tokachi-Oki earthquake of 1968, *Bull. Seism. Soc. Am.* **68**, 767–779.
- Omote, S., K. Ohmatsuzawa, and T. Ohta (1980). Recently developed strong motion earthquake instruments array in Japan, *Proc. 7th World Conf. Earthquake Eng.*, Vol. 2, Istanbul, Turkey, 8–13 September, 41–48.
- Project Team for the Development of Small-Size Long-Period Seismometer (1974). Development of the portable easy-operation long-

- period seismometer (PELS Type 73), Part. 1, *Special Bull. Earthquake Res. Inst. Univ. Tokyo* **13**, 17–22 (in Japanese with English abstract).
- Seo, K., K. Hamada, and F. Kaneko (1990). Underground structure in Saitama Prefecture as derived from explosion seismic prospecting (programs and abstracts), *Seism. Soc. Japan* **2**, 94 (in Japanese).
- Shiono, K., Y. Ohta, and K. Kudo (1979). Observation of 1- to 5-sec microtremors and their application to earthquake engineering. Part 5, existence of Rayleigh wave components, *Zisin (J. Seism. Soc. Japan)* **32**, 115–124 (in Japanese with English abstract).
- Toshinawa, T. and T. Ohmachi (1992). Love wave propagation in a three-dimensional sedimentary basin, *Bull. Seism. Soc. Am.* **82**, 1661–1677.
- Vidale, J. E. and D. V. Helmberger (1988). Elastic finite difference modeling of the 1971 San Fernando, California, earthquake, *Bull. Seism. Soc. Am.* **78**, 122–141.
- Yamanaka, H., K. Seo, and T. Samano (1992a). Analysis and numerical modeling of surface-wave propagation in a sedimentary basin, *J. Phys. Earth* **40**, 57–71.
- Yamanaka, H., M. Kamata, M. Takemura, and K. Takahashi (1992b). Characteristics of long-period ground motion in the northwestern Kanto plain, *Summaries of Technical Papers of Annual Meeting Architectural Institute of Japan*, Vol. B1, Niigata, Japan, 417–418 (in Japanese).
- Yamanaka, H., M. Dravinski, and H. Kagami (1993). Continuous measurements of microtremors on sediments and basement in Los Angeles, California, *Bull. Seism. Soc. Am.* **83**, 1595–1609.
- Kobori Research Complex, Kajima Corporation
6-5-30 Akasaka, Minato-ku, Tokyo 107, Japan
(H.Y., M.T.)
- Kajima Technical Research Institute, Kajima Corporation
19-1, Tobitakyu 2-Chome, Chofu-shi, Tokyo 182, Japan
(H.I., M.N.)

Manuscript received 3 January 1994.